Mantle upwelling and initiation of rift segmentation beneath the Afar Depression

Mantle upwelling and initiation of rift segmentation beneath the Afar Depression

J.O.S. Hammond[1,2], J.-M. Kendall[2], G.W. Stuart[3], C.J. Ebinger[4], I.D. Bastow[1], D. Keir[5], A. Ayele[6], M. Belachew[4,6], B. Goitom[7], G. Ogubazghi[7,8], and T.J. Wright[3]

[1]Department of Earth Science and Engineering, Imperial College London, SW7 2AZ London, UK
[2]School of Earth Sciences, University of Bristol, BS8 1RJ Bristol, UK
[3]School of Earth and Environment, University of Leeds, Leeds, West Yorkshire LS2 9JT, UK
[4]Department of Earth and Environmental Sciences, University of Rochester, Rochester, New York 14611, USA
[5]National Oceanography Centre, Southampton, University of Southampton, Southampton, Hampshire SO14 3ZH, UK
[6]Institute of Geophysics, Space Science and Astronomy, Addis Ababa University, Addis Ababa, Ethiopia
[7]Department of Earth Sciences, Eritrea Institute of Technology, Asmara, Eritrea
[8]Department of Physics, University of Botswana, Gabrone, Botswana

ABSTRACT

The Afar Depression, at the northern end of the East African Rift, is the only place on land where the transition from a plume-induced continental breakup to seafloor spreading is active today. New images of seismic velocity structure, based on exceptional new data sets, show that the mantle plume that initiated rifting in Africa is absent beneath Afar today. The images are dominated by a major low-velocity feature at ~75 km depth closely mimicking the abrupt changes in rift axis orientation seen at the surface. This is likely associated with passive upwelling beneath the rift. Additional focused low-velocity anomalies show that small diapiric upwellings are present beneath major off-axis volcanoes. These multiple melting sources can explain the wide range of geochemical signatures seen in Afar. These images suggest that passive upwelling beneath Afar marks the initiation of rift segmentation as continental breakup progresses to seafloor spreading.

INTRODUCTION

It has long been suggested that hot upwelling material from deep in the Earth may have instigated rifting in East Africa (Willis, 1936; White and McKenzie, 1989), and causes the dynamic uplift of much of the African continent (Ebinger and Sleep, 1998; Lithgow-Bertelloni and Silver, 1998). Yet, how upwelling material interacts with the lithosphere and uppermost asthenosphere beneath the African plate is still a matter of debate. Previous studies have imaged continuous low velocities extending from the core-mantle boundary beneath southern Africa and reaching the surface beneath the thinnest lithosphere in Afar, Ethiopia (Hansen et al., 2012), supporting the idea that mantle material flows northward (Ebinger and Sleep, 1998). Others propose that upwelling material may be sourced from other areas of the lower mantle closer to Afar (Montagner et al., 2007; Chang and Van der Lee, 2011). Conversely, recent seismic imaging and numerical models imply that the depth of melting beneath Afar is consistent with decompression melting and no significant thermal anomaly is required at present (Rychert et al., 2012). High $^{3}He/^{4}He$ ratios in Oligocene flood basalts suggest a lower mantle source, yet Neogene–Holocene lavas indicate increasing dilution of the lower mantle contributions by upper mantle sources (Pik et al., 2006), suggesting that the plume influence has weakened over time. Seismic tomography of the upper mantle can test these models of mantle circulation, but existing seismic images of the mantle beneath the Afar Depression lack adequate resolution. Seismic images of mantle structure beneath the narrow, weakly extended Main Ethiopian Rift show low-velocity zones near steep lithosphere-asthenosphere gradients beneath the rift flanks (Bastow et al., 2008), but it remains unclear how mantle structure changes in the broadly rifted Afar Depression. Here we present data from five new seismic experiments in Afar and the surrounding highlands (Fig. 1) that, combined with existing data from the Main Ethiopian Rift, allow us to produce seismic tomographic inversions with lateral resolution of ~50 km. For the first time we can address how upwelling material interacts with the shallow mantle beneath Afar, and how melt production in the mantle supplies the incipient spreading center segments at the surface.

RELATIVE TRAVELTIME TOMOGRAPHY

We use data from 244 seismic stations across Ethiopia, Eritrea, Djibouti, Yemen, and Kenya (Fig. 1; Table DR1 in the GSA Data Repository[1]). We pick P-wave and S-wave traveltimes from teleseismic arrivals recorded by five new seismic experiments in northern Ethiopia (Ebinger et al., 2008; Belachew et al., 2011; Hammond et al., 2011) and Eritrea (Fig. 1) and have repicked all available legacy data (Benoit et al., 2006; Bastow et al., 2008; Montagner et al., 2007) (Fig. 1). In total, 1088 earthquakes were analyzed (Fig. 1; Table DR2), resulting in 10,999 P/PKP-wave and 13,161 S/SKS-wave traveltime picks. This allows us to produce a seismic model for the top 400 km beneath Afar with unprecedented resolution (~50 km). The data are inverted using a standard regularized, linear least squares inversion method (VanDecar et al., 1995), jointly inverting for slowness, near-surface corrections, and earthquake corrections (see the Data Repository).

SEISMIC VELOCITY MODELS

Previous studies have found low velocities (–1.5% for P-waves, –2.5% for S-waves) beneath the Main Ethiopian Rift (Bastow et al., 2008). With our increased seismic network coverage, we show that comparable low velocities are found in the upper mantle beneath Afar (Fig. 2). The S-wave model shows a striking low-velocity feature beneath almost the total length of the rift axis (Fig. 2), mimicking the abrupt changes in rift axis orientation at the surface, whereas the P-wave models show a more discontinuous structure, particularly in northern Afar, where focused (~50 km width) low-velocity material is offset by ~70 km to the east and ~20 km to the west of the rift axis and is close to sharp gradients in topography at the lithosphere-asthenosphere boundary (Hammond et al., 2011; Rychert et al., 2012) (Fig. 2). Synthetic checkerboard tests (Fig. DR2 in the Data Repository) show that we can resolve features of ~50 km scale well with our inversion scheme. The strong low velocities extend to depths of 200 km where the magnitude of the low-velocity anomalies decreases (–1.0% for P-waves, –2.0% for S-waves) and the wavelength of the anomaly increases (Fig. 2). This change in mantle structure is not an artifact of resolution, as we can resolve features ~50 km in size at these depths (Fig. DR2). The western Ethiopia plateau region, characterized by chains of recent eruptive centers, is underlain by low velocities, whereas

[1]GSA Data Repository item 2013175, Tables DR1 and DR2, Figures DR1–DR4 and description of methods, is available online at www.geosociety.org/pubs/ft2013.htm, or on request from editing@geosociety.org or Documents Secretary, GSA, P.O. Box 9140, Boulder, CO 80301, USA.

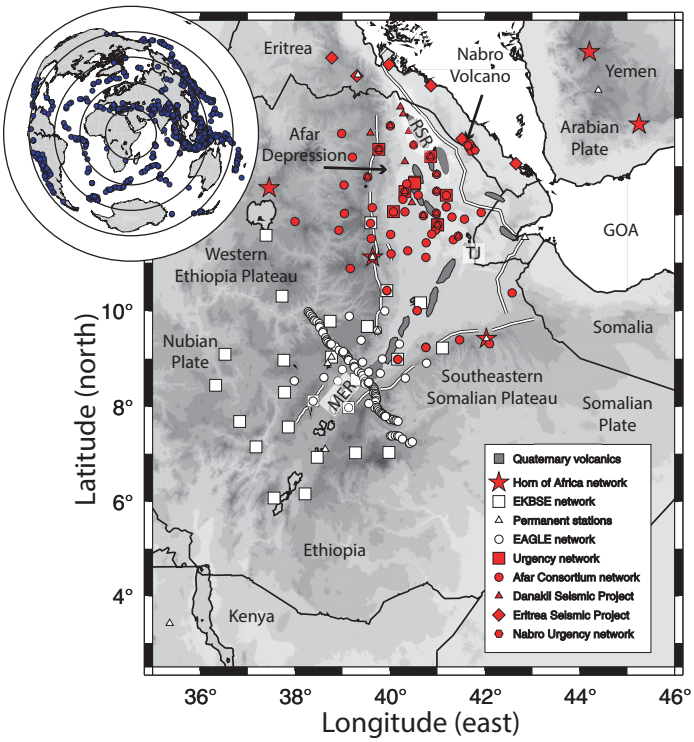

Figure 1. Map showing earthquakes and seismic stations used in the tomographic inversion. Solid white lines show major faults bounding Afar Depression, gray filled regions show Quaternary volcanic segments, and black lines show political borders. MER—Main Ethiopian Rift, GOA—Gulf of Aden, RSR—Red Sea Rift, TJ—triple junction, EAGLE—Ethiopia Afar Geoscientific Lithospheric Experiment, EKBSE—Ethiopia Kenya Broadband Seismic Experiment. Red symbols show data used in tomography for first time, white symbols show stations used in previous studies (Benoit et al., 2006; Bastow et al., 2008).

faster velocities are seen away from the recent eruptive centers beneath the northernmost Ethiopian Highlands, and on the southeastern Somalian plateau (Fig. 2).

DISCUSSION

The strong low velocities in the uppermost 200 km have previously been linked to melt that feeds volcanism beneath the Main Ethiopian Rift (Bastow et al., 2008). Our images support this idea with the lowest velocities underlying young magmatic segments and regions of thinned crust with high bulk crustal V_p/V_s indicative of melt in the lower crust (Hammond et al., 2011) (Fig. 2). Petrology (Rooney et al., 2005), receiver function studies (Rychert et al., 2012), and seismic anisotropy (Kendall et al., 2006) suggest that the melting zone is in the top 75–90 km beneath the rift. Our tomographic images, in contrast, show low velocities down to ~200 km. However, synthetic modeling resolves the apparent discrepancy, showing that a model containing just low-velocity material beneath the rift in the top 90 km would be smeared to depths of 150–200 km, with a reduction in the anomaly strength from −10% to ~−3% and ~−2.5% for P-waves and S-waves, respectively (Figs. DR3 and DR4).

In general, the lowest velocities are directly below the segmented and irregular rift axis, indicating that along-axis segmentation is in part maintained by shallow passive mantle upwelling. The most likely cause of partial melt is decompression melting beneath the progressively widening zones of thinned lithosphere. The low velocities are most pronounced in the S-wave models, which show larger amplitude anomalies (~−2.5%) compared to the P-wave models (~−1.5%). This difference in amplitudes is not due to resolution, where we can resolve amplitudes at these depths better for P-waves than S-waves (Figs. DR2–DR4). S-wave velocities are more sensitive to melt than P-waves. The lower crust and upper mantle beneath Afar contain appreciable amounts of melt, giving rise to high V_p/V_s (>2.0) deduced from receiver function studies (Hammond et al., 2011), and low S-wave velocities derived from surface-wave studies (Guidarelli et al., 2011). The differences in P-wave and S-wave anomalies

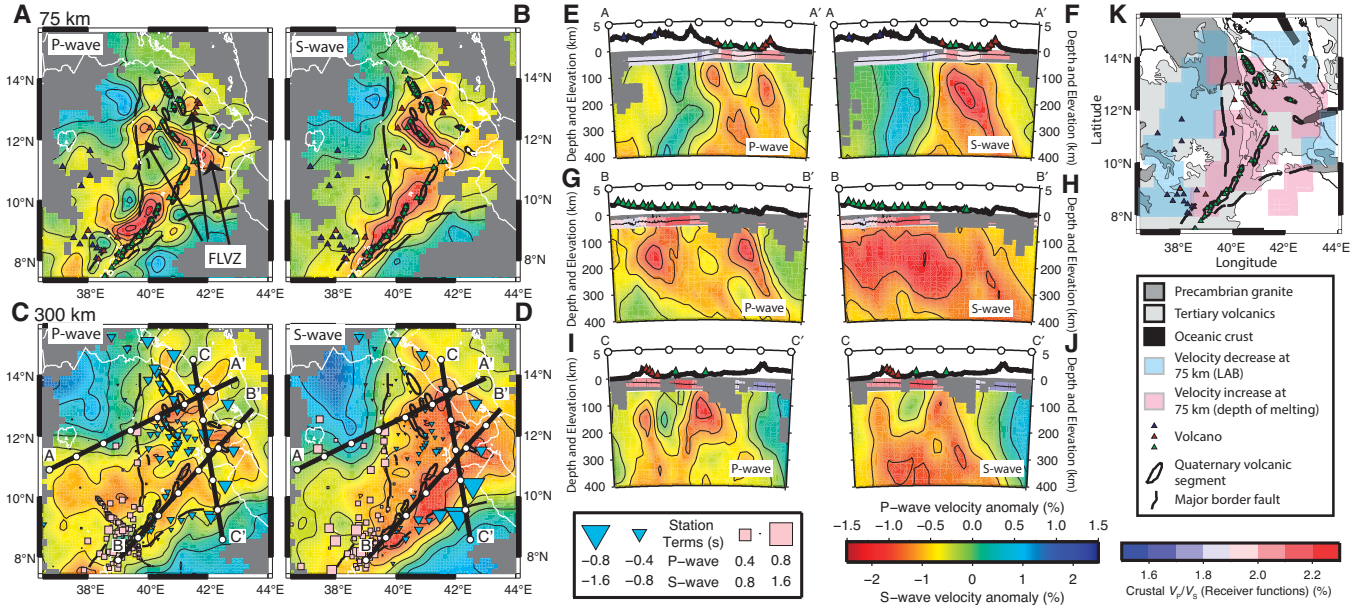

Figure 2. A: Depth slice at 75 km for P-wave model. B: Depth slice at 75 km for S-wave model. C: Depth slice at 300 km for P-wave model. D: Depth slice at 300 km for S-wave model. (Inverted blue triangles and red squares show the station terms.) E–J: Cross sections related to the profiles shown in C and D. Cross sections also show topography and crustal thickness profiles. Colors in crustal thickness profiles relate to bulk crustal velocity, V_p/V_s (Hammond et al., 2011). Regions shaded gray mask out areas with <10 rays in each node. FLVZ—focused low-velocity zones. E, G, and I are cross sections for P-waves; F, H, and J are cross sections for S-waves. K: Simplified geological map of Afar and surrounding regions, and locations of velocity decrease at 75 km (lithosphere-asthenosphere boundary, LAB; blue) and regions of velocity increase at 75 km (depth of melting, pink) (Rychert et al., 2012). Regions not shaded pink or blue show absence of signal related to either LAB or depth of melting. Blue triangles show volcanoes older than Quaternary, red triangles show significant off-axis Quaternary volcanoes, and green triangles show Quaternary volcanoes close to rift axis.

in the presence of melt are even more pronounced when melt retains a preferential orientation, as has been proposed to explain mantle seismic anisotropy beneath the Main Ethiopian Rift and Red Sea Rift (Kendall et al., 2006; Gao et al., 2010).

S-wave receiver functions show a strong velocity increase with depth across most of Afar at ~75 km depth (Rychert et al., 2012). This is inferred to show the base of the melting column, which is at a depth similar to that of mid-oceanic ridge basalt–generation zones worldwide, and does not require a large thermal anomaly. Petrological estimates of mantle temperatures in Afar are sparse, but samples from the last 10 m.y. show a range of temperature estimates (1370–1494 °C); the higher values suggest a hotter mantle beneath Afar, yet are considerably lower than other plume-affected mantle worldwide (Rooney et al., 2012). Our upper mantle models show some along-axis variability, consistent with passive upwelling beneath the broad Afar Rift zone spreading centers, modulated by relatively small temperature fluctuations.

There are three regions in Afar where strong low velocities exist in the P-wave models that are not present in the S-wave models. These are close to the western margin (12.5°N, 40°E), Nabro volcano in the vicinity of the Danakil microplate (13°N, 42°E), and the triple junction region (11.5°N, 42°E) (labeled FLVZ, focused low-velocity zones, in Fig. 2). These low-velocity zones are adjacent to relatively unrifted crust compared to most of the Afar Depression (Hammond et al., 2011), and regions of steep gradients in lithosphere-asthenosphere boundary depth (Rychert et al., 2012) (Fig. 2), where some models predict enhanced melt production (Holtzman and Kendall, 2010). In addition, the correlation with off-axis volcanoes is consistent with enhanced melt generation (Fig. 2). However, the presence of enhanced melt should cause stronger S-wave anomalies relative to P-wave anomalies. We suggest that the P-wave models resolve localized thermal anomalies, whereas the S-wave models are dominated by melt-related anomalies so that thermal anomalies are not resolvable in Afar. While steep gradients in lithosphere-asthenosphere boundary topography may enhance melt at these locations, focused diapiric thermal upwellings from the upper mantle may be present, causing localized deeper melt zones. This may explain the presence of elevated mantle temperatures seen in the petrology (Rooney et al., 2012), while satisfying the seismic constraint for a regional depth of melting consistent with little thermal anomaly (Rychert et al., 2012). This is supported by the absence of a velocity increase with depth at 75 km seen in the S-wave receiver functions (Rychert et al., 2012) (Fig. 2).

Below 200 km to at least depths of 400 km, we show P-wave and S-wave anomalies that are generally weaker (–1.0% for P-waves, –2.0% for S-waves), and have a longer dominant wavelength (Fig. 2). The complex structures present in the top 100–200 km are absent below 200 km.

Given the 40 m.y. history of flood basalt magmatism in Ethiopia (Hofmann et al., 1997), a broad plume head would likely have dissipated, and the scales of the low-velocity zones are too broad and complex for a plume stem predicted by classical models (Griffiths and Campbell, 1990). This broad feature with little coherent structure below 200 km has previously been linked to the African superplume (Benoit et al., 2006; Bastow et al., 2008; Hansen et al., 2012). This is further supported by measurements of seismic anisotropy (Kendall et al., 2006; Gao et al., 2010) that are consistent with flow from the southwest. However, the easternmost Afar–Red Sea region shows some structure at deeper depths with larger low-velocity S-wave anomalies below 200 km. These low velocities are located close to lower mantle upwellings seen in regional tomographic models (Montagner et al., 2007; Chang and Van der Lee, 2011), and close to the region of hottest temperatures determined petrologically (Rooney et al., 2012). While it is likely that the African superswell dominates flow in the mantle, a further upwelling impinging beneath Arabia and arriving from the northeast cannot be ruled out (Chang and Van der Lee, 2011).

Regardless of where the deeper material is sourced, it is clear that as mantle material rises beneath Afar, it is focused into smaller features on the scale of 50–100 km that may signal the onset of centrally fed, along-axis mantle upwellings maintaining second-order mid-ocean ridge segmentation (Keir et al., 2009). Similar regularly spaced, focused, low-velocity zones, interpreted as upwellings, are seen beneath the youthful Gulf of California (Mexico) plate boundary (Wang et al., 2009). These may correspond to zones of increased melt production or reduced density of depleted mantle beneath the spreading center. Plate reconstructions and petrological and geophysical studies indicate high degrees of plate thinning within the central Afar Depression, and the long-lived magmatic intrusions produce a crustal composition transitional between continental and oceanic (Hammond et al., 2011). Yet, intense periods of multiple dike injections sourced from crustal magma reservoirs at the centers of ~50-km-long faulted zones that mark the narrow zone of active extension show dimensions and processes nearly identical to those observed at spreading ridges (Hayward and Ebinger, 1996; Belachew et al., 2011; Wright et al., 2012), and paired magnetic anomalies in Afar (Courtillot et al., 1980; Bridges et al., 2012) that may indicate the earliest stage of seafloor spreading.

We interpret the broad zone of low-velocity upper mantle beneath the Main Ethiopian Rift, Afar, and the western Ethiopian plateau as evidence for buoyant upwelling from the deeper mantle, which contributes several hundred meters of relief to the observed topography (Ebinger and Sleep, 1998; Lithgow-Bertelloni and Silver, 1998). In Afar, the strong correlation between the narrow low S-wave velocity zones and the active rift segments, the absence of continental lithosphere (Rychert et al., 2012), as well as the magnitude of the velocity anomalies suggest that these are zones of localized asthenospheric upwelling supplying centrally fed magmatic segments. Additional localized low-velocity zones exist in the P-wave models, and are marked at the surface by relatively unfaulted large volcanoes, increased temperatures, and enhanced melt extraction zones in three regions with steep lithosphere-asthenosphere boundary gradients along the trailing edges of the relatively thick continental lithosphere (Rooney et al., 2012; Rychert et al., 2012) (Fig. 3).

IMPLICATIONS

Our tomographic models show that a classical plume with a narrow stem and broad head does not currently exist beneath Afar. The uppermost mantle (<100 km) is dominated by passive upwelling beneath the

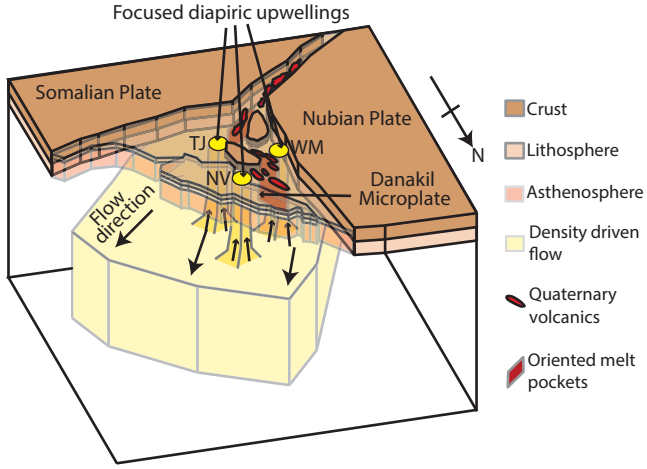

Figure 3. Proposed model where passive upwelling of asthenosphere in mantle beneath Afar, Ethiopia, gives rise to melt-filled mantle above 75 km (Rychert et al., 2012), with melt oriented at rift axis causing significant seismic anisotropy (Kendall et al., 2006; Gao et al., 2010) and large velocity anomalies. Superimposed on this are focused diapiric thermal upwellings. These focused anomalies cause enhanced melting at three locations: triple junction (TJ), Nabro volcano (NV), and western margin (WM).

narrow active rift segments, overprinted by focused diapiric upwellings. These localized features cause enhanced melting beneath the triple junction, western margin, and Nabro volcano; this, when superimposed with the incipient passive upwellings beneath the new oceanic lithosphere, can explain the range of geochemical signatures (Pik et al., 2006; Rooney et al., 2012) and the broad distribution of active eruptive centers. The narrow low-velocity zones, showing passive upwelling beneath magmatic segments with persistent crustal magma reservoirs near their centers, signal the initiation of buoyancy-driven flow driving along-axis segmentation (Phipps Morgan and Chen, 1993) as Afar approaches seafloor spreading.

ACKNOWLEDGMENTS

We thank Addis Ababa University, the Eritrea Institute of Technology, the Afar National Regional State Government, Ethiopia, and the Southern Red Sea Region Administration, Eritrea, for support throughout the various experiments. The facilities of SEIS-UK are supported by the Natural Environment Research Council (NERC) under Agreement R8/H10/64. Seismic instruments were also supplied by the Incorporated Research Institutions for Seismology (IRIS) Program for Array Seismic Studies of the Continental Lithosphere (PASSCAL). The facilities of the IRIS Consortium are supported by the U.S. National Science Foundation (NSF) under Cooperative Agreement EAR-0552316 and by the U.S. Department of Energy National Nuclear Security Administration. Funding was provided by NERC grants NE/E007414/1, NE/D008611/1, and NE/J012297/1, NSF grant EAR-0635789, and BHP-Billiton. Hammond is supported by NERC Fellowship NE/I020342/1, Bastow is supported by the Leverhulme Trust, and Wright is supported by a Royal Society University Research Fellowship.

REFERENCES CITED

Bastow, I.D., Nyblade, A.A., Stuart, G.W., Rooney, T.O., and Benoit, M.H., 2008, Upper mantle seismic structure beneath the Ethiopian hot spot: Rifting at the edge of the African low-velocity anomaly: Geochemistry Geophysics Geosystems, v. 9, Q12022, doi:10.1029/2008GC002107.

Belachew, M., Ebinger, C., Coté, D., Keir, D., Rowland, J.V., Hammond, J.O.S., and Ayele, A., 2011, Comparison of dike intrusions in an incipient seafloor spreading segment in Afar, Ethiopia: Seismicity perspectives: Journal of Geophysical Research, v. 116, B06405, doi:10.1029/2010JB007908.

Benoit, M.H., Nyblade, A.A., and VanDecar, J.C., 2006, Upper mantle P-wave speed variations beneath Ethiopia and the origin of the Afar hotspot: Geology, v. 34, p. 329–332, doi:10.1130/G22281.1.

Bridges, D.L., Mickus, K., Gao, S.S., Abdelsalam, M.G., and Alemu, A., 2012, Magnetic stripes of a transitional continental rift in Afar: Geology, v. 40, p. 203–206, doi:10.1130/G32697.1.

Chang, S.J., and Van der Lee, S., 2011, Mantle plumes and associated flow beneath Arabia and East Africa: Earth and Planetary Science Letters, v. 302, p. 448–454, doi:10.1016/j.epsl.2010.12.050.

Courtillot, V., Galdeano, A., and Le Mouel, J.L., 1980, Propagation of an accreting plate boundary: A discussion of new aeromagnetic data in the Gulf of Tadjurah and southern Afar: Earth and Planetary Science Letters, v. 47, p. 144–160, doi:10.1016/0012-821X(80)90113-2.

Ebinger, C.J., and Sleep, N.H., 1998, Cenozoic magmatism throughout East Africa resulting from impact of a single plume: Nature, v. 395, p. 788–791, doi:10.1038/27417.

Ebinger, C.J., Keir, D., Ayele, A., Calais, E., Wright, T.J., Belachew, M., Hammond, J.O.S., Campbell, E., and Buck, W.R., 2008, Capturing magma intrusion and faulting processes during continental rupture: Seismicity of the Dabbahu (Afar) rift: Geophysical Journal International, v. 174, p. 1138–1152, doi:10.1111/j.1365-246X.2008.03877.x.

Gao, S., Liu, K., and Abdelsalam, M., 2010, Seismic anisotropy beneath the Afar Depression and adjacent areas: Implications for mantle flow: Journal of Geophysical Research, v. 115, B12330, doi:10.1029/2009JB007141.

Griffiths, R.W., and Campbell, I.H., 1990, Stirring and structure in mantle starting plumes: Earth and Planetary Science Letters, v. 99, p. 66–78, doi:10.1016/0012-821X(90)90071-5.

Guidarelli, M., Stuart, G., Hammond, J.O.S., Kendall, J.M., Ayele, A., and Belachew, M., 2011, Surface wave tomography across Afar, Ethiopia: Crustal structure at a rift triple-junction zone: Geophysical Research Letters, v. 38, L24313, doi:10.1029/2011GL046840.

Hammond, J.O.S., Kendall, J.-M., Stuart, G.W., Keir, D., Ebinger, C., Ayele, A., and Belachew, M., 2011, The nature of the crust beneath the Afar triple junction: Evidence from receiver functions: Geochemistry Geophysics Geosystems, v. 12, Q12004, doi:10.1029/2011GC003738.

Hansen, S.E., Nyblade, A.A., and Benoit, M.H., 2012, Mantle structure beneath Africa and Arabia from adaptively parameterized P-wave tomography: Implications for the origin of Cenozoic Afro-Arabian tectonism: Earth and Planetary Science Letters, v. 319–320, doi:10.1016/j.epsl.2011.12.023.

Hayward, N.J., and Ebinger, C.J., 1996, Variations in along-axis segmentation of the Afar rift system: Tectonics, v. 15, p. 244–257, doi:10.1029/95TC02292.

Hofmann, C., Courtillot, V., Féraud, G., Rochette, P., Yirgu, G., Ketefo, E., and Pik, R., 1997, Timing of the Ethiopian flood basalt event and implications for plume birth and global change: Nature, v. 389, p. 838–841, doi:10.1038/39853.

Holtzman, B.K., and Kendall, J.M., 2010, Organized melt, seismic anisotropy and plate boundary lubrication: Geochemistry Geophysics Geosystems, v. 11, Q0AB06, doi:10.1029/2010GC003296.

Keir, D., and 13 others, 2009, Evidence for focused magmatic accretion at segment centers from lateral dike injections captured beneath the Red Sea rift in Afar: Geology, v. 37, p. 59–62, doi:10.1130/G25147A.1.

Kendall, J.M., Pilidou, S., Keir, D., Bastow, I.D., Stuart, G.W., and Ayele, A., 2006, Mantle upwellings, melt migration and the rifting of Africa: Insights from seismic anisotropy, *in* Yirgu, G., et al., eds., The Afar Volcanic Province within the East African Rift System: Geological Society of London Special Publication 259, p. 55–72, doi:10.1144/GSL.SP.2006.259.01.06.

Lithgow-Bertelloni, C., and Silver, P.G., 1998, Dynamic topography, plate driving forces and the African superswell: Nature, v. 395, p. 269–272, doi:10.1038/26212.

Montagner, J.-P., Marty, B., Stutzmann, E., Sicilia, D., Cara, M., Pik, R., Lévêque, J.-J., Roult, G., Beucler, E., and Debayle, E., 2007, Mantle upwellings and convective instabilities revealed by seismic tomography and helium isotope geochemistry beneath eastern Africa: Geophysical Research Letters, v. 34, L21303, doi:10.1029/2007GL031098.

Phipps Morgan, J., and Chen, Y.J., 1993, Dependence of ridge-axis morphology on magma supply and spreading rate: Nature, v. 364, p. 706–708, doi:10.1038/364706a0.

Pik, R., Marty, B., and Hilton, D.R., 2006, How many mantle plumes in Africa? The geochemical point of view: Chemical Geology, v. 226, p. 100–114, doi:10.1016/j.chemgeo.2005.09.016.

Rooney, T., Furman, T., Yirgu, G., and Ayalew, D., 2005, Structure of the Ethiopian lithosphere: Xenolith evidence in the Main Ethiopian Rift: Geochimica et Cosmochimica Acta, v. 69, p. 3889–3910, doi:10.1016/j.gca.2005.03.043.

Rooney, T., Herzberg, C., and Bastow, I.D., 2012, Elevated mantle temperature beneath East Africa: Geology, v. 40, p. 27–30, doi:10.1130/G32382.1.

Rychert, C.A., Hammond, J.O.S., Harmon, N., Kendall, J.M., Keir, D., Ebinger, C., Bastow, I.D., Ayele, A., Belachew, M., and Stuart, G., 2012, Volcanism in the Afar rift sustained by decompression melting with minimal plume influence: Nature Geoscience, v. 5, p. 406–409, doi:10.1038/ngeo1455.

VanDecar, J.C., James, D.E., and Assumpacao, M., 1995, Seismic evidence for a fossil mantle plume beneath South America and implications for plate driving forces: Nature, v. 378, p. 25–31, doi:10.1038/378025a0.

Wang, Y., Forsyth, D.W., and Savage, B., 2009, Convective upwelling in the mantle beneath the Gulf of California: Nature, v. 462, p. 499–501, doi:10.1038/nature08552.

White, R., and McKenzie, D., 1989, Magmatism at rift zones—The generation of volcanic continental margins and flood basalts: Journal of Geophysical Research, v. 94, p. 7685–7729, doi:10.1029/JB094iB06p07685.

Willis, B., 1936, East African plateaus and rift valleys: Washington, D.C., Carnegie Institute of Washington, 358 p.

Wright, T.J., and 12 others, 2012, Geophysical constraints on the dynamics of spreading centres from rifting episodes on land: Nature Geoscience, v. 5, p. 242–250, doi:10.1038/ngeo1428.

Manuscript received 3 August 2012
Revised manuscript received 19 December 2012
Manuscript accepted 8 January 2013

Printed in USA